Influence of Different Filling Materials on Stiffness of a New Buffer Bag

HOU Yu[1], *ZHANG Ming*[2], *NIE Hong*[1*]

1. Key Laboratory of Fundamental Science for National Defense-Advanced Design Technology of Flight Vehicle, Nanjing University of Aeronautics & Astronautics, Nanjing 210016, P. R. China;
2. State Key Laboratory of Mechanics and Control of Mechanical Structures, Nanjing University of Aeronautics and Astronautics, Nanjing 210016, P. R. China

(Received 19 November 2020; revised 17 January 2021; accepted 24 January 2021)

Abstract: A buffer bag mechanism is designed, which can provide axial impact protection under small displacement. The stiffness characteristics of the structure under impact load are studied. The stiffness of the mechanism and the internal pressure change of the buffer bag are compared and analyzed, when the filling materials are liquid and gas respectively. Finally, the influence of initial fluid bag pressure, bulk modulus and shell thickness on the stiffness of the mechanism and the change of bag pressure are studied. The results show that the stiffness of the liquid bag is better than that of the gas bag when the filler is liquid and gas; the liquid bag has obvious pressure rise after the mechanism is subjected to axial force by 300 kN, and the gas bag has almost no pressure rise; the change of bulk modulus, which is 1 000, 1 500, 2 000 and 2 500 MPa, has an obvious effect on the liquid bag, and it is positively correlated with the stiffness of the mechanism. The change of gas modulus, which is 28 and 44, has little effect on the stiffness of the mechanism; the thickness of the buffer bag, which is 5, 10 and 15 mm, also has an obvious effect on the stiffness. The stiffness of the liquid bag is greater, and the protection for flexible joint is better in the same condition.

Key words: buffer bag; flexible joint; axial protection; liquid bag; gas bag

CLC number: TH135 **Document code:** A **Article ID:** 1005-1120(2021)01-0106-11

0 Introduction

With the continuous growth of industrial demand, the research and application of buffer at home and abroad is becoming more and more mature[1-3]. Traditional hydraulic buffer has such a complex structure that cannot support large load under small displacement and deformation, which limits its application in practice. The traditional shock absorber is not suitable for small displacement and small deformation. Therefore, a new type of buffer bag is designed to provide small displacement and deformation of axial impact protection in the mechanism[4]. Buffer bag is a kind of non-metallic buffer which is filled with fluid in a flexible closed container and uses the buffer property of fluid to work. The buffer bag can absorb a lot of energy in small deformation and recover quickly. The flexible and easy to deform composite material is used in the contact part of the buffer device and the mechanism, which can fit well with the mechanism under the impact load, so as to prevent the damage of the mechanism caused by stress concentration. So far, liquid buffer bag has been rarely investigated at home and abroad. However, buffer airbag and air spring similar to liquid buffer bag have been studied in depth[5-10]. The rigid and unique characteristics of the gas bag and the liquid bag are better, and need to be further studied under the same condition, as well as the buffer performance of them[11].

In this paper, a kind of buffer bag cushion is chosen, and the influence of different filling materi-

*Corresponding author, E-mail address: hnie@nuaa.edu.cn.

How to cite this article: HOU Yu, ZHANG Ming, NIE Hong. Influence of different filling materials on stiffness of a new buffer bag[J]. Transactions of Nanjing University of Aeronautics and Astronautics, 2021, 38(1): 106-116.

http://dx.doi.org/10.16356/j.1005-1120.2021.01.010

als on the stiffness characteristics of the buffer bag is studied when the filling is gas or liquid. The axial stiffness characteristics of the buffer bag are further addressed.

1 Working Process of Buffer Bag

1.1 Buffer bag shock absorber

The mechanism of shock absorber is mainly composed of two parts: one is rubber joint, and the other is buffer bag, as shown in Fig.1(a). When the mechanism works, a large axial upward impact load is exerted at the bottom of the mechanism[12].

The flexible joint is composed of laminated elastic layer and metal layer. The metal plate and rubber layer are bonded together, and thus there is no large axial static displacement. Otherwise, the flexible joint may fail and cause the mechanism failure. Therefore, it is necessary to use large stiffness damper to protect the rubber joint axially. It is assumed that there is absolute adhesion between the elastic layer and the metal one. The schematic diagram of the flexible joint is shown in Fig.1(b).

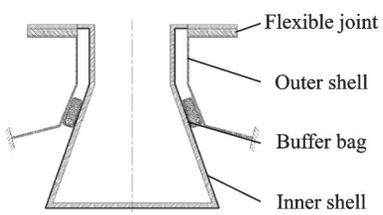

(a) Mechanism model

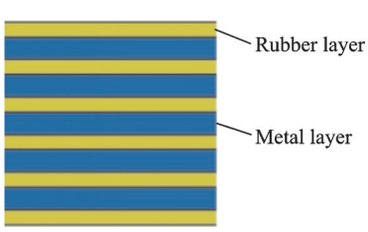

(b) Rubber joint model

Fig.1 Buffer bag shock absorption mechanism

As shown in Fig.2(a), the buffer bag is a kind of conical ring flexible sealing container filled with incompressible fluid. The real buffer bag is not connected in the loop upward, and the head end and tail end of the buffer bag have a closed ring, which is inserted with a hinge pin to lock the buffer bag in the mechanism. The pressure pipe is connected with the joint and the bottom of the buffer bag to realize the charging of the buffer bag, and the joint is connected with the pressure filling device.

The pressure of the buffer bag can be adjusted to a predetermined value, and the buffer bag can be placed between the inner and outer shells of the mechanism, which can greatly reduce the load transmitted to the rubber joint through the contact area between the inner and outer shells. The simplified model of the buffer bag is shown in Fig.2(b).

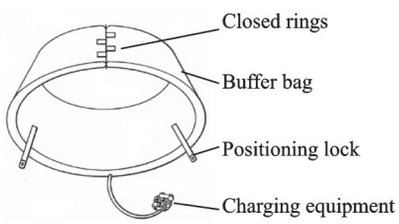

(a) Buffer bag

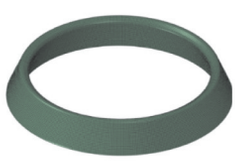

(b) Simplified model of buffer bag

Fig.2 Schematic of buffer bag and its simplified model

1.2 Numerical method for analyzing buffer bag

When the liquid reaches the static equilibrium state in the buffer bag, there is no tension and tangential force between the liquid particles, as well as between the liquid and buffer bag. Only the normal pressure exists, which is the hydrostatic pressure of the fluid[13]. The hydrostatic pressure of the liquid acting on any point of the buffer bag is the same in each direction, and it is not related to the normal direction of the pressure action surface, that is, not related to the shape of the buffer bag. Since the liquid in the buffer bag is a continuous medium, the hydrostatic pressure is a continuous function related to the spatial coordinate. Hence, the following equation can be obtained.

$$p=f(x,y,z) \tag{1}$$

A small parallelepiped is randomly selected from the liquid in the buffer bag. The sides of the six faces are dx, dy and dz, which are parallel to the

three coordinate axes. Let the projection of unit mass force on the coordinate axis be f_x, f_y, f_z. The components of mass force in x, y and z axes are $\rho f_x \mathrm{d}x\mathrm{d}y\mathrm{d}z$, $\rho f_y \mathrm{d}x\mathrm{d}y\mathrm{d}z$, and $\rho f_z \mathrm{d}x\mathrm{d}y\mathrm{d}z$. The surface force is hydrostatic pressure. If the hydrostatic pressure of the fluid at any point in the hexahedron is p, the hydrostatic pressure at the center of the two surfaces parallel to the x-axis in the normal direction is divided into

$$p - \frac{\mathrm{d}x}{2}\frac{\partial p}{\partial x}\ ,\ p + \frac{\mathrm{d}x}{2}\frac{\partial p}{\partial x} \tag{2}$$

The hexahedron is a small hexahedron. Therefore, the average hydrostatic pressure in the plane can be regarded as equal to the pressure at the central point. Therefore, the hydrostatic pressure of the fluid on these two surfaces are

$$\left(p - \frac{\mathrm{d}x}{2}\frac{\partial p}{\partial x}\right)\mathrm{d}y\mathrm{d}z\ ,\ \left(p + \frac{\mathrm{d}x}{2}\frac{\partial p}{\partial x}\right)\mathrm{d}y\mathrm{d}z \tag{3}$$

Since the sum of all the external force vectors acting on the hexahedron is 0, it can be known that for the x-axis

$$\rho f_x \mathrm{d}x\mathrm{d}y\mathrm{d}z + \left(p - \frac{\mathrm{d}x}{2}\frac{\partial p}{\partial x}\right)\mathrm{d}y\mathrm{d}z - \left(p + \frac{\mathrm{d}x}{2}\frac{\partial p}{\partial x}\right)\mathrm{d}y\mathrm{d}z = 0 \tag{4}$$

After simplification, the following results can be obtained.

$$f_x - \frac{\partial p}{\rho \partial x} = 0 \tag{5}$$

Similarly, similar results can be obtained on the y and z axes. Then, when the liquid in the buffer bag is in equilibrium, the differential equations are as follows

$$\begin{cases} f_x - \dfrac{\partial p}{\rho \partial x} = 0 \\ f_y - \dfrac{\partial p}{\rho \partial y} = 0 \\ f_z - \dfrac{\partial p}{\rho \partial z} = 0 \end{cases} \tag{6}$$

According to Eq.(6), when the liquid in the buffer bag is at rest, the change rate of hydrostatic pressure along any axis is equal to its unit mass force. In the buffer bag, compared with the external force, the pressure change caused by the liquid mass force is negligible. In Eq.(6), f_x, f_y, f_z can thus be regarded as 0. Therefore, the following results are obtained.

$$\frac{\partial p}{\partial x} = 0,\ \frac{\partial p}{\partial y} = 0,\ \frac{\partial p}{\partial z} = 0 \tag{7}$$

This means that the change rate of hydrostatic pressure of the liquid in the buffer bag along any axis is 0, that is, the pressure in the buffer bag is equal everywhere. The shell and liquid of the buffer bag are divided into fine grids by finite element method. Since the liquid pressure is equal everywhere, the pressure of each liquid unit is also the same. The volume (density) of liquid is related to temperature and pressure. In this paper, all the liquid units form a set, and set a reference point (RP) for this set. The initial pressure and density of all liquid units are given at the RP, and then the real simulation of the buffer bag is completed.

2 Stiffness Analysis of Buffer Bag

2.1 Finite element model for buffer bag mechanism analysis

2.1.1 Coupling of buffer bag and material properties

According to the structural characteristics of the buffer bag damping mechanism, the mechanical analysis model of the buffer bag cushion system is established by using ABAQUS[14]. S4R mesh is used to define buffer bag, inner shell and shell, and C3D8 element is used to define flexible joint. It is assumed that both the mass and temperature of the fluid in the bag remain unchanged[15]. The fluid cavity method is used to couple the buffer bag at the RP[16]. The fluid cavity method in ABAQUS can be used to calculate the gas (liquid)-structure interaction based on the surface defined fluid strength (the filling can be liquid or gas). When defining the fluid cavity, the properties of the filling in the fluid cavity can be defined by the RP, where the RP has coupling with the fluid cavity. Subsequently, set the

properties of the liquid at RP-1, as shown in Fig. 3. The material of buffer mechanism is high strength steel. The buffer bag is made of rubber fiber. Table 1 is relevant material properties.

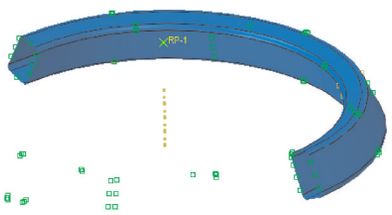

Fig.3 Coupling whit fluid cavity method

Table 1 Material properties of model

Material	Density/(tonne·mm^{-3})	Elastic modulus/MPa	Poisson's ratio	Bulk modulus/MPa	Molecular mass/(tonne·mol^{-1})
High strength steel	7.8×10^{-9}	2.1e+05	0.3	N/A	N/A
Compound material	1.4×10^{-9}	7.0e+03	0.3	N/A	N/A
Water	1.0×10^{-9}	N/A	N/A	2.18e+03	N/A
Air	1.2×10^{-12}	N/A	N/A	N/A	2.8e−05

2.1.2 Simulation of contact

When the buffer bag is compressed, the contact states among inner, outer shell and buffer bag change with its deformation. In ABAQUS, this kind of contact is treated as finite-sliding interaction between deformable bodies, where separation and sliding of finite amplitude and arbitrary rotation of the surfaces may arise. Defining possible contact conditions by identifying and pairing potential contact surfaces, the appropriate contact elements are generated automatically. To define a sliding interface between two surfaces, one of the surfaces is the "slave" surface. The other surface is the "master" surface. Two contact pairs were defined in this paper. The first contact pair, the outer surface of inner shell, i.e., the master surface, and inner diameter surface of bag, i.e., the slave surface, are shown in Fig.4. The second contact pair, the inner surface of outer shell, i.e., the master surface, and outer diameter surface of bag, i.e., the slave surface, are shown in Fig. 5.

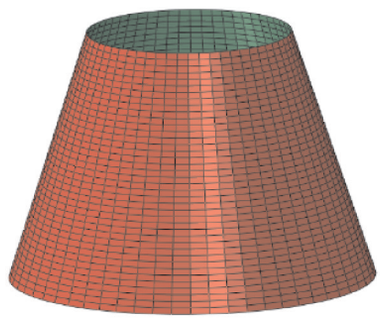

(a) Outer surface of inner shell

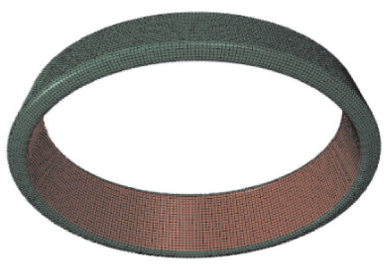

(b) Inner diameter surface of bag

Fig.4 Master surface and slave surface for the first contact pair

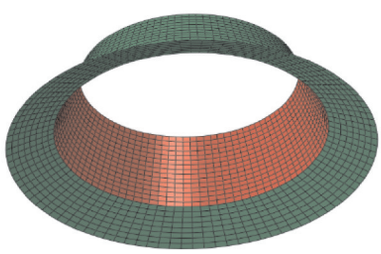

(a) Inner surface of outer shell

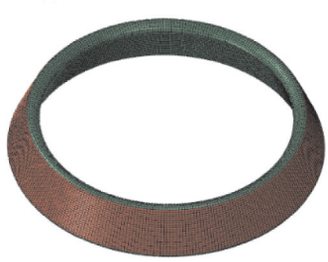

(b) Outer diameter surface of bag

Fig.5 Master surface and slave surface for the second contact pair

2.1.3 Boundary conditions and mesh independence test

In the real working state of the buffer bag, the mechanism will be subjected to strong impact load. Typical external input curve is shown in Fig.6. The

load is exerted on the bottom of the mechanism in a short period of time, and gradually decreases afterwards. The concentrated load is set to act on the bottom of the inner shell, and the load acts on the load coupling reference node in the model, so that the load is distributed on the bottom surface of the inner shell, as shown in Fig. 7. The initial pressure of the buffer bag is 1.5 MPa, and the impact load on the bottom of inner shell is 300 kN. Before the formal loading, the buffer bag was pressurized to 1.5 MPa. Then, the inner shell was released and the impact load was formally applied.

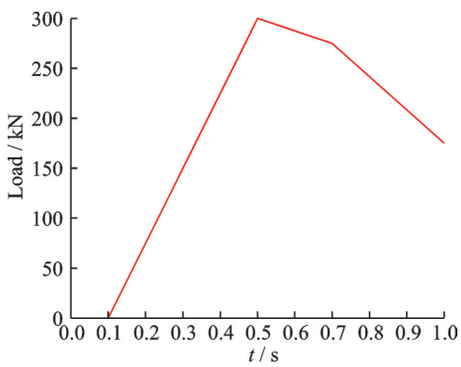

Fig.6 External input curve

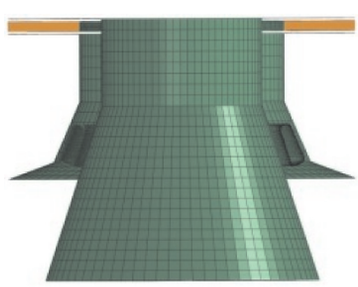

(a) Finite element model of mechanism

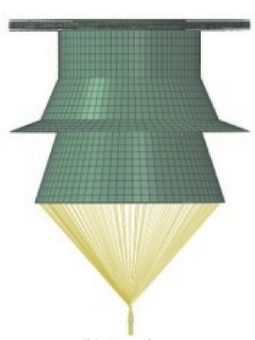

(b) Load case

Fig.7 Finite element model

Mesh independence test is an important task of FEA. Table 2 shows the analysis of mesh independence test. Considering the accuracy and time, 10 mm mesh size is chosen.

Table 2 Mesh independence test

Mesh size/mm	2.5	5	10	20
Maximum stress of liquid bag / MPa	22.7	22.8	22.6	17.8
Time of liquid bag / s	663	421	327	246
Maximum stress of gas bag / MPa	19.9	19.9	19.6	17.1
Time of gas bag / s	931	375	313	261

2.2 Result analyses of different filling materials

2.2.1 Result analysis of gas bag

As shown in Fig. 8, the stress map of the gas bag and the displacement map of the flexible joint can be obtained by analyzing the mechanical characteristics of the gas bag buffer system after establishing the real simulation model of the gas bag system. It can be seen from Fig.8(a) that under the action of load, the inner shell axis moves upward, the gas bag deforms with the axial displacement of the inner shell, and the stress map is evenly distributed in the circumferential direction. On the surface of the gas bag, the stress is concentrated in the lower part of the inner side of gas bag and the upper part of the outer side of gas bag. The maximum stress is located in the top part of the outside of gas bag, as shown in Fig. 8(b). In the process of impact loading, it can be seen that the displacement of flexible joint is small, and it is well protected in the whole deformation process.

The dynamic stress map of gas bag within 0.0—1.1 s after applied the impact load is shown in Fig.9. The results show that during the dynamic deformation process, the stress map is evenly distributed in the circumferential direction, and the stress is larger in the lower and upper parts of the gas bag. During the loading process of impact load, the stress of gas bag increases gradually and reaches its peak value about 0.5 s. Then the stress on the gas bag decreases.

Fig. 10 is the stress curve of the node with the largest stress value in the gas bag from 0.0 s to 1.1 s. The results show that in the initial stage of 0.0—0.1 s, the process is the filling stage of convective

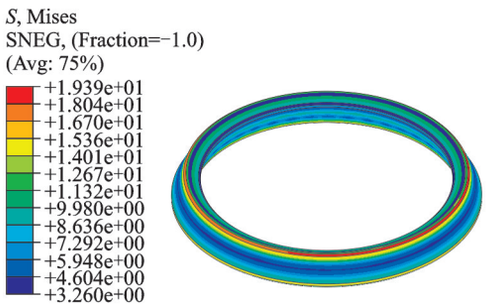

(a) Stress map of gas bag

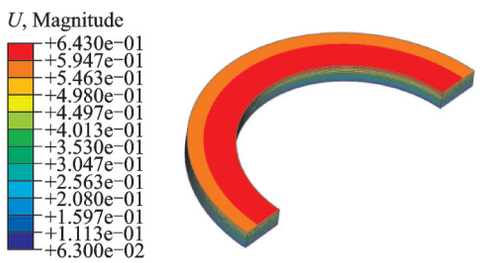

(b) Displacement map of flexible joint

Fig.8 Stress map of the gas bag and displacement map of the flexible joint

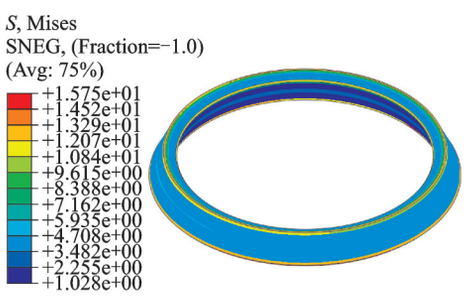

(a) 0.1 s

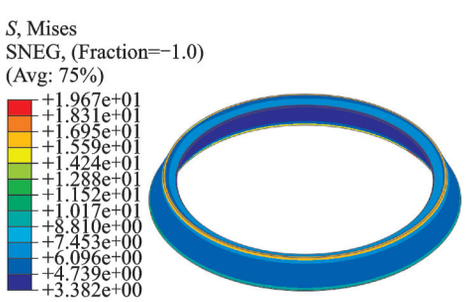

(b) 0.5 s

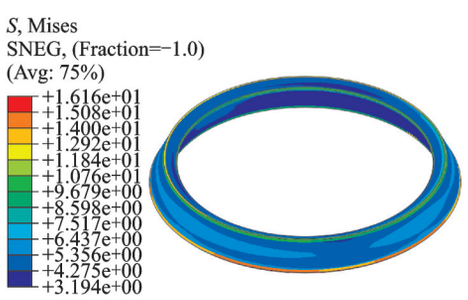

(c) 1.1 s

Fig.9 Stress map of gas bag dynamic process

bag. When the pressure of fluid bag increases from 0.0 MPa to 1.5 MPa, the node stress will rapidly increase to a fixed value; In the stage of 0.1—0.3 s, due to the existence of initial pressure of 1.5 MPa, the stress is in dynamic oscillation state at this stage with the increase of load, and the stress does not increase significantly. At the stage of 0.3—0.5 s, the stress of the node increases with the increase of load, and reaches the maximum value at 0.5 s, where the load is also maximal. At the stage of 0.5—1.1 s, the load began to decrease, and the stress of the joint also began to decrease. At 1.1 s, the load becomes half of the maximum value, and the stress value of the node is smaller than the value in the oscillation stage.

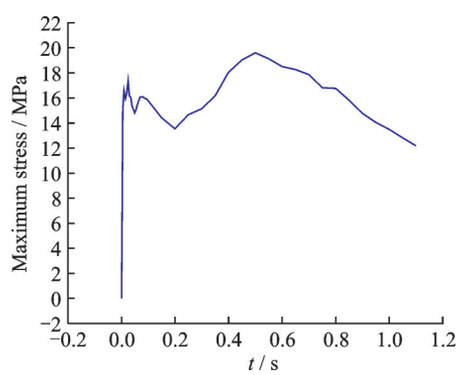

Fig.10 Maximum stress curve of gas bag element

2.2.2 Result analysis of liquid bag

Fig.11 is the stress map of the liquid bag and the displacement map of the flexible joint, where the filler is water. It can be seen that the liquid bag deforms with the axial displacement of the inner shell. Compared with Fig.8(a), the stress map is also uniformly distributed in the circumferential direction, and the position of the maximum stress on the surface of the liquid bag is on the outer edge at the top of the outside of liquid bag. It can be seen from Fig.11(b) that the displacement map is uniformly distributed in the circumferential direction after the impact load. The maximum displacement position is also close to the interior, and the external displacement is small. It implies that the buffer liquid bag has strong resistance to deformation.

The dynamic stress map of liquid bag within 0.0—1.1 s after applied the impact load is shown in Fig.12. Compared with Fig.9, it shows that during

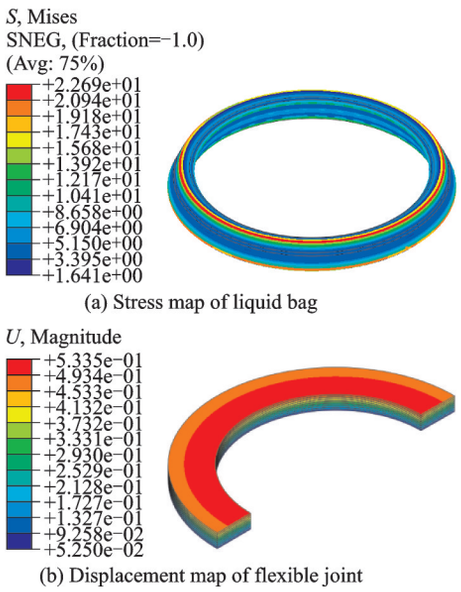

Fig.11 Stress map of liquid bag and displacement map of flexible joint

the dynamic deformation process, the stress map is evenly distributed in the circumferential direction, and the stress is larger in the lower and upper parts of the fluid bag. During the loading process of impact load, the stress of fluid bag increases gradually and reaches its peak value of 0.5 s approximately. Then the stress on the fluid bag decreases.

Fig. 13 is the stress curve of the node with the largest stress value in the fluid bag from 0.0 s to 1.1 s. Compared with Fig. 10, it shows that in the initial stage of 0.0—0.1 s, the process is the filling stage of convective bag. When the pressure of fluid bag increases from 0.0 MPa to 1.5 MPa, the node stress will rapidly increase to a fixed value, which is same as Fig.10. In the stage of 0.1—0.3 s, due to the existence of initial pressure of 1.5 MPa, the stress is in dynamic oscillation state at this stage with the increase of load, and the stress does not increase significantly, which is same as Fig.10. At the stage of 0.3—0.5 s, compared with Fig.10, the stress of the node increases slowly with the increase of load, and reaches the maximum value 22 MPa at 0.5 s and the load at the same time. At the stage of 0.5—1.1 s, the load began to decrease, and the stress of the joint also began to decrease. At 1.1 s, the load becomes half of the maximum value. Compared with

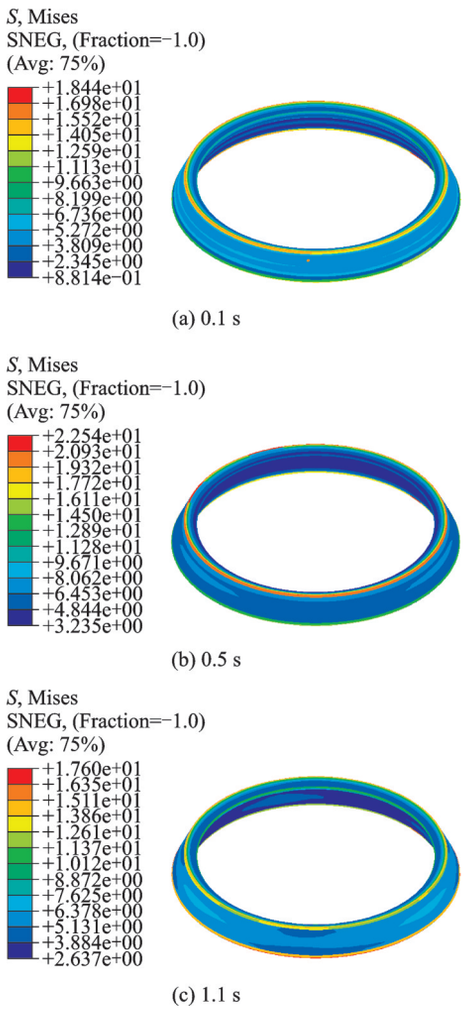

Fig.12 Stress map of fluid bag dynamic process

Fig. 10, the stress value of the node returns to the same value as that of the oscillation stage.

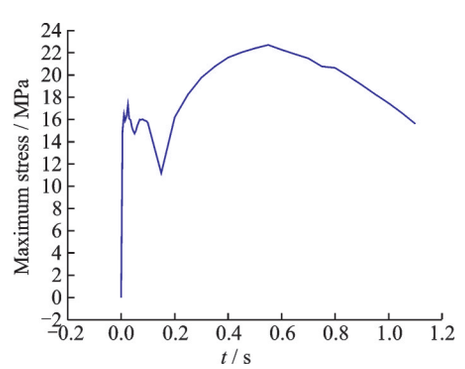

Fig.13 Maximum stress curve of liquid bag element

Fig. 14 is the simulated distance of the buffer bag under impact load. By comparing with the relevant experimental data obtained by Zhang et al.[4], it can be found that the simulation model is in good agreement with the experimental structure.

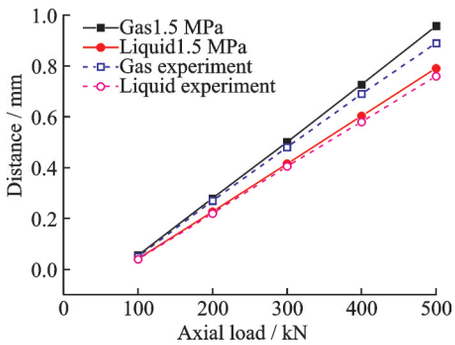

Fig.14 Simulated and experimental distance of gas bag and liquid bag

2.3 Influence of different parameters on stiffness of buffer bag

2.3.1 Influence of initial pressure of buffer bag

The axial displacement of the flexible joint is calculated when the initial pressure of the buffer bag is 1.5, 2.0, 2.5 and 3.0 MPa, and the calculation results are shown in Fig.15(a). It can be seen from Fig.15(a) that when the internal fillers are gas and liquid, the external load and axial displacement are in positive proportion. When the initial pressure is different, the axial displacement decreases with the increase of initial pressure. Compared with gas and liquid, the axial displacement of liquid bag is smaller than that of gas bag under the same conditions, that is, the stiffness of the liquid bag is larger and deformation is smaller.

When the initial pressure of the buffer bag is different, the internal pressure change of the buffer bag is calculated, and the results are shown in Fig.15(b). According to Fig.15(b), when the internal filling material is liquid, the internal pressure of the liquid bag increases with the increase of external load, and the increase is more obvious. When the inner filler is gas, the internal pressure of the gas bag hardly changes with the increase of external load.

2.3.2 Influence of bulk modulus of buffer bag

The axial displacement of the flexible joint is calculated when the initial pressure of the buffer bag is 1.5 MPa, the gas modulus is 28 and 44, and the liquid elastic modulus is 1 000, 1 500, 2 000 and

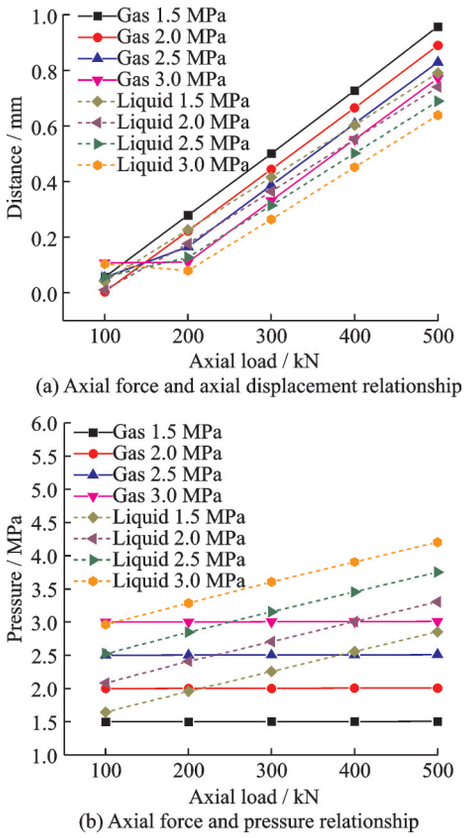

Fig.15 Influence of initial pressure of buffer bag

2 500 MPa. The calculation results are shown in Fig.16(a). When the filler is gas, the geometry of the stiffness curve does not change when the gas modulus is different. that is, the influence of the gas modulus on the stiffness of the mechanism can be ignored. When the filler is liquid, the stiffness of the mechanism increases with the increase of the elastic modulus of the liquid, showing a positive correlation. Comparing the stiffness curves of gas and liquid, it is found that the stiffness of liquid is greater than that of gas.

When the initial pressure is 1.5 MPa, the internal pressure changes of the buffer bag under different gas modulus and different liquid elastic modulus are calculated. The calculation results are shown in Fig.16(b). When the internal filler is liquid, the internal pressure of the liquid bag increases with the increase of the elastic modulus of the liquid, and the increased value is nonlinear. When the inner filler is gas, the internal pressure of the gas bag hardly changes with the increase of external load.

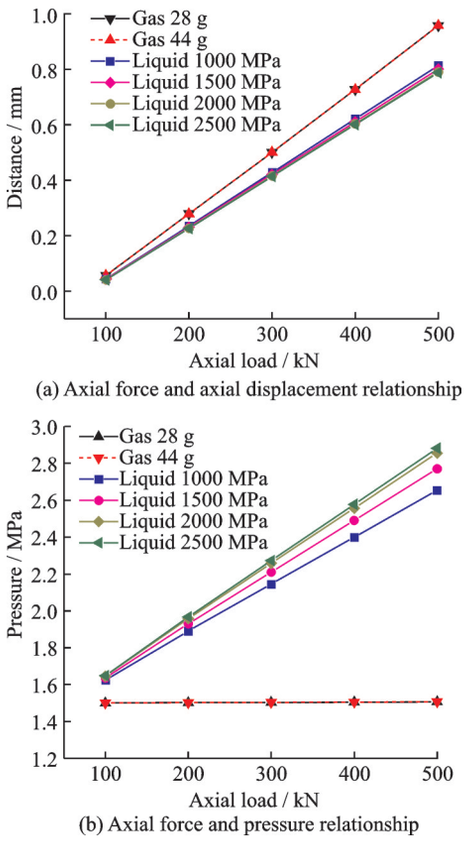

Fig.16 Influence of bulk modulus of buffer bag

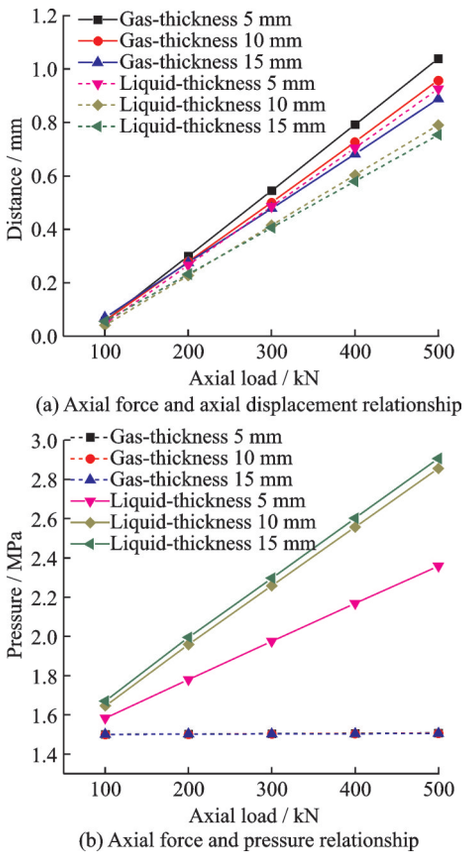

Fig.17 Influence of buffer bag thickness

2.3.3 Influence of buffer bag thickness

The initial pressure is 1.5 MPa, and the thickness is 5, 10 and 15 mm. The stiffness of the buffer bag with different thickness is calculated, and the calculation results are shown in Fig. 17(a). When the initial pressure is the same and the filler is gas and liquid, the stiffness of the structure will increase with the increase of the thickness. Compared with gas and liquid, the axial stiffness of liquid bag is greater than that of gas bag.

The initial pressure is 1.5 MPa, and the pressure change of buffer bag with different thickness is calculated. The calculation results are shown in Fig.17(b). When the internal filling material is liquid, the pressure of the liquid bag increases with the increase of the thickness, and the relationship is nonlinear. When the inner filling is gas, the pressure of the gas bag almost does not change with the increase of the thickness.

3 Conclusions

In this paper, the mechanical properties of buffer bag are studied. The influence of gas bag and liquid bag on the stiffness of the buffer mechanism is analyzed. Finally, the effects of initial pressure, bulk modulus and thickness on the stiffness of the mechanism are studied

(1) After the mechanism is impacted by 300 kN, the displacement change is very small, which indicates that the buffer bag has a good protection on the flexible joint under the impact load. After comparing and analyzing the liquid bag and the gas bag, it is found that after the mechanism is subjected to axial force, the liquid bag has obvious pressure rise, and the internal pressure of the gas bag hardly changes.

(2) The influence of initial pressure, bulk modulus and thickness of buffer bag on the stiffness of the mechanism are discussed. It is found that the change of bulk modulus (1 000, 1 500, 2 000 and 2 500 MPa) has an obvious effect on the liquid bag, so it is positively correlated with the stiffness of the mechanism. The change of gas modulus (28 and 44) has little effect on the stiffness of the mecha-

nism. The thickness of the buffer bag (5 mm, 10 mm and 15 mm) also has an obvious effect on the stiffness. The gas bag and the liquid bag show different changing rules under different thickness conditions.

(3) Through the overall stiffness analysis and observation of the pressure change of the buffer bag, it can be known that the stiffness of the liquid bag is greater under the same condition, and it has better protection for flexible joint.

Reference

[1] TUTT B, SANDY C, CORLISS J. Status of the development of an airbag landing system for the orion crew module: AIAA 2009-2923[R]. USA: AIAA, 2009: 1-13

[2] ERIN C, WILSON B, ZAPFE J. An improve model of a pneumatic vibration isolator: Theory and experiment[J]. Journal of Sound & Vibration, 1998, 218(1): 81-101.

[3] BERG M. A nonlinear rubber spring model for rail vehicle dynamics analysis[J]. Vehicle System Dynamics, 1998, 30(3/4): 197-212.

[4] ZHANG Ming, JIANG Rui, NIE Hong. Analysis of stiffness characteristics of a new fluid bag for axial shock protection[J]. Journal of Vibroengineering, 2015, 17(2): 587-601.

[5] BERG M. A three dimensional airspring model with friction and orifice damping[J]. Vehicle System Dynamics Supplement, 1999(33): 528-539.

[6] ODA N, NISHIMURA S. Vibration of air suspension bogies and their design[J]. JSME International Journal, 2008, 13(55): 43-50.

[7] LI Xuebing, HE Yuan, LIU Wanqiang, et al. Research on the vertical stiffness of a rolling lobe air spring[J]. Proceedings of the Institution of Mechanical Engineers, Part F: Journal of Rail and Rapid Transit, 2016, 230(4): 1172-1183.

[8] YUASA T, SAKAI T, HOSOYA H, et al. Application of CAE in the development of air suspension beam[J]. Circulation Journal Official Journal of the Japanese Circulation Society, 1997, 67(1): 93-103.

[9] LEE H W, HUH H. Finite element analysis of air springs with fiber-reinforced rubber composites using 3-D shell elements[J]. Transactions of the Korean Society of Mechanical Engineers A, 2001, 25(4): 602-609.

[10] LEE H W, KIM S H, HUH H, et al. Finite element analysis of diaphragm type air springs with fiber-reinforced rubber composites[J]. Journal of Composite Materials, 2003, 37(14): 1261-1274.

[11] OMAN S, NAGODE M. The influence of piston shape on air-spring fatigue life[J]. Fatigue and Fracture of Engineering Materials and Structures, 2017, 41(8): 1019-1031.

[12] WONG P K, XIE Zhengchao, ZHAO Jing, et al. Analysis of automotive rolling lobe air spring under alternative factors with finite element model[J]. Journal of Mechanical Science and Technology, 2014, 28(12): 5069-5081.

[13] LI Yan, HE Lin, SHUAI Changgeng, et al. Improved hybrid isolator with maglev actuator integrated in air spring for active-passive isolation of ship machinery vibration[J]. Journal of Sound and Vibration, 2017(407): 226-239.

[14] LI Xuebing, WEI Yintao, HE Yuan. Simulation on polytropic process of air springs[J]. Engineering Computations, 2016, 33(7): 1957-1968.

[15] ZHU Hengjia, YANG J, ZHANG Yunqing, et al. A novel air spring dynamic model with pneumatic thermodynamics, effective friction and viscoelastic damping[J]. Journal of Sound and Vibration, 2017(408): 87-104.

[16] HEINRICH N, DONNER H, IHLEMANN J. Evaluation of air spring textile reinforcement by means of resolving the cord structure in FE analyses [J]. Proceedings in Applied Mathematics and Mechanics, 2017, 17(1): 305-306.

Acknowledgements This work was supported by the Fundamental Research Funds for the Central Universities (No. NS2019003).

Authors Dr. **HOU Yu** received the M.S. degree in Aircraft Design and Engineering from Nanjing University of Aeronautics and Astronautics, China, in 2016, and he is studying for the Ph.D. degree in Aircraft Design from Nanjing University of Aeronautics and Astronautics, China, starting from 2017. His current research interests include aircraft design, FEA and landing gear system.

Prof. **NIE Hong** received the Ph.D. degree in Aircraft Design from Nanjing University of Aeronautics and Astronautics, Nanjing, China, in 1992. Now he is a professor in Nanjing University of Aeronautics and Astronautics. His current research interests include aircraft design, dynamics and landing gear system.

Author contributions Prof. **NIE Hong** designed the study and raised the idea. Dr. **HOU Yu** assisted in writing the manuscript. Prof. **ZHANG Ming** contributed to the data for the analysis, and the discussion and background of the study. All authors commented on the manuscript draft and approved the submission.

Competing interests The authors declare no competing interests.

(Production Editor: ZHANG Tong)

不同填充材料对新型缓冲囊刚度的影响

侯 聿[1], 张 明[2], 聂 宏[1]

(1.南京航空航天大学飞行器先进设计技术国防重点学科实验室,南京 210016,中国; 2.南京航空航天大学机械结构力学及控制国家重点实验室,南京 210016,中国)

摘要:设计了一种能在小位移下提供轴向冲击保护的新型缓冲囊机构,并研究了该结构在冲击载荷作用下的刚度特性。通过比较分析填充材料分别为液体和气体时,机构的刚度和缓冲囊内部压力的变化,讨论了初始囊内压力、体积模量和囊壁厚对机构刚度以及囊内压力变化的影响。结果表明,当填料分别为液体和气体时,液囊的刚度优于气囊;当机构承受300 kN轴向力后,液囊的内部压力有明显的上升,而气囊的内压几乎没有上升;液囊内液体体积模量的改变(分别为1 000、1 500、2 000和2 500 MPa时)对机构刚度有明显影响,且与机构刚度呈正相关;气体摩尔质量的变化(分别为28和44时)对机构的刚度影响不大;缓冲囊的壁厚(分别为5、10和15 mm时)对机构的刚度也有明显的影响。相同条件下,液囊的缓冲刚度较大,对柔性接头的保护更好。

关键词:缓冲囊;柔性接头;轴向保护;液囊;气囊